Realizing a topological transition in a non-Hermitian quantum walk with circuit QED

Yizhou Huang,[1] Zhang-qi Yin,[1,*] and W. L. Yang[2]

[1]*Center for Quantum Information, Institute for Interdisciplinary Information Sciences, Tsinghua University, Beijing 100084, China*

[2]*State Key Laboratory of Magnetic Resonance and Atomic and Molecular Physics, Wuhan Institute of Physics and Mathematics, Chinese Academy of Sciences, Wuhan 430071, China*

(Received 19 January 2016; published 3 August 2016)

We extend the non-Hermitian one-dimensional quantum walk model [Phys. Rev. Lett. **102**, 065703 (2009)] by taking the dephasing effect into account. We prove that the feature of topological transition does not change even when dephasing between the sites within units is present. The potential experimental observation of our theoretical results in the circuit QED system consisting of superconducting qubit coupled to a superconducting resonator mode is discussed and numerically simulated. The results clearly show a topological transition in quantum walk and display the robustness of such a system to the decay and dephasing of qubits. We also discuss how to extend this model to higher dimension in the circuit QED system.

DOI: 10.1103/PhysRevA.94.022302

I. INTRODUCTION

As a quantum analog of the well-known classical random walk, quantum walk serves as a fascinating framework for various quantum information processes, such as basic search [1], universal quantum computation [2], quantum measurement [3], etc. Apart from its numerous applications, quantum walk also displays new traits different from its classical counterpart, such as the fast spreading of the wave function compared to a classical random walk [4], which was used for explaining the high-efficiency photosynthetic energy transfer assisted by environment [5–8]. Reference [9] considered a one-dimensional (1D) quantum walk on a bipartite lattice, where a topological transition was discovered and experimental implementation in quantum dots or cavity QED (CQED) was briefly discussed. In it, the environment effect was included by using a non-Hermitian Hamiltonian, as done in Ref. [10]. Later, the same model was extended to multidimensional systems [11].

As shown in Fig. 1, the quantum walk could be realized on a 1D bipartite indexed lattice where decay sites (blue) and nondecay sites (white) appear in turn. The strengths of hopping between sites are characterized by v (within the same unit) and v' (between neighboring units). Due to it, a random "walker" starting from a nondecay site of unit m_0 may end up decaying from the system from another unit m with probability P_m. Given the relative strengths of v and v', the average displacement of a "walker"

$$\sum_m m \cdot P_m - m_0 \tag{1}$$

before it decays is quantized as an integer (0 for $v' < v$ and -1 for $v' > v$) no matter what the decay coefficient $\gamma > 0$ is. It is worthwhile to note that the average displacement would be

$$-\frac{v'}{v' + v} \tag{2}$$

if the system is classical and hoppings are incoherent. One can derive this from the symmetry of the system. [12]

As shown in Ref. [13], such system displayed parity-time symmetry [14–16]. These different displacements correspond to unbroken and broken parity-time symmetry regimes and display a topological transition.

In this work we will show that such transition is robust even in the presence of qubit dephase. Note that this idea can be experimentally realized in a CQED setting, where a qubit is coupled to one resonator mode [17,18]. Specifically the two states of the qubit ($|e\rangle$, $|g\rangle$) represent two sites of the same unit, where the higher-energy qubit state ($|e\rangle$) has decay rate γ. The cavity photon number state $|n\rangle$ represents the nth unit. Here we suppose that the cavity decay κ is much less than qubit decay γ, therefore we neglect it. Such a system could be an atom in a cavity coupled to one cavity mode, or similarly as CQED systems: a superconducting Josephson junction which acts as a qubit coupled to a lumped LC oscillator in a superconducting electric circuit. Recently, circuit QED systems have attracted a lot of attention as they could be easily scaled up and controlled [19]. We will stick to the circuit QED system setup henceforth.

On the other hand, an experiment realized bipartite non-Hermitian quantum walk in optical waveguide [20], which in essence is a classical simulation of a quantum effect. However, the non-Hermitian quantum walk in circuit QED is fully quantum. Another merit of a circuit QED system is that extending to higher dimension quantum walk is relatively easy, as a high-dimensional quantum walk can be implemented by coupling the qubit to more than one resonator mode. We will show features of the quantum walk that emerge with the growth of dimensionality.

In Sec. II we explained in detail the system setup and the properties of the effective Hamiltonian of the system. In Sec. III we extend the analytical theory in Ref. [9] to accommodate the existence of dephase, and show that the qubit dephase, one major source of decoherence in normal circuit QED systems, will not affect the topological structure experimentally observed. In Sec. IV we carried out numerical calculations for different parameters of the system, including the preparation of the system, the decay rate of the qubit, the detuning of the system, and the effect of qubit dephasing. In Sec. V we extended this model to higher dimensions of bipartite quantum walk and carried out numerical calculations

*yinzhangqi@mail.tsinghua.edu.cn

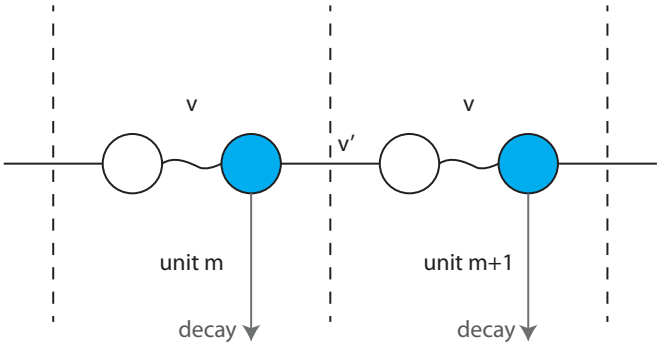

FIG. 1. Non-Hermitian quantum walk model. A particle can hop between the nearest sites with strength v or v' depending on whether that hop crosses unit boundaries. When the particle is on the blue sites, it would decay with rate γ.

for a two-dimensional (2D) quantum walk specifically. We will show that such quantum walk realization is feasible in circuit QED setting, and a good topological transition can be observed with a modest requirement on the system parameters aforementioned.

II. THE CIRCUIT QED MODEL

We consider a system where a two-level qubit is coupled to a resonator mode, with external microwave driving. Such a system can be expressed in a standard circuit QED Hamiltonian

$$H_{\text{org}} = g(\sigma^+\tilde{a} + \sigma^-\tilde{a}^\dagger) + \Omega/2(\sigma^+ + \sigma^-) + \tfrac{1}{2}\Delta\epsilon\sigma^z, \qquad (3)$$

where σ^z,$\sigma^\pm$ are Pauli operators for the qubit, g characterizes the coupling strength, and $\tilde{a}(\tilde{a}^\dagger)$ are lowering (rising) operators on the resonator mode in a rotating frame, $\Delta\epsilon$ is (real) detuning of the system and consists of the energy differences between the two states of the qubit minus the minimum energy gap for the resonator, and Ω is the Rabi frequency of external drive on the atom. We use subscript "org" to distinguish this Hamiltonian from the effective Hamiltonian H that we will put forward later.

To consider the dissipation of the system, we consider only qubit decay and dephase. We use γ to characterize qubit decay rate and d for qubit dephase rate. The master equation of the system is

$$\dot{\rho}(t) = -i[H_{\text{org}},\rho(t)] + d[\sigma^z\rho(t)\sigma^z - \rho(t)] + \frac{\gamma}{2}[2\sigma^-\rho(t)\sigma^+ - \sigma^+\sigma^-\rho(t) - \rho(t)\sigma^+\sigma^-]. \qquad (4)$$

In the usual experimental setup [21], the strength of cavity decay is at the magnitude of ∼1 kHz or less, which is significantly smaller than other parameters in the system, such as the coupling strength g, which could reach ∼100 MHz, and qubit decay γ is on the order of MHz. Therefore, we ignore the cavity decay effects. Besides, the external drive Ω is easily tunable to fulfill the topological transition conditions.

Experimentally, one can detect qubit decay by either a photon detector or ways discussed later in this section, but generally one cannot detect qubit dephasing from leaking photons. Furthermore, the setup of this experiment requires immediate measurement of cavity photon number upon qubit decay, which could be realized by detecting photon emission with photon detectors. Therefore, we treated qubit decay and dephase differently. We follow the quantum jump approach in Ref. [22] and put the qubit decay term into the Hamiltonian, which yields an effective non-Hermitian Hamiltonian

$$H = g(\sigma^+\tilde{a} + \sigma^-\tilde{a}^\dagger) + \Omega/2(\sigma^+ + \sigma^-) + \frac{1}{2}\Delta\epsilon\sigma^z - \frac{i\gamma}{2}|e\rangle\langle e|. \qquad (5)$$

The details of this derivation are in the Appendix. Then the Lindblad master equation of the system would be [23]

$$\dot{\rho}(t) = -i[H,\rho(t)] + d[\sigma^z\rho(t)\sigma^z - \rho(t)]. \qquad (6)$$

Ideally, if the system is initialized at photon number state $|N\rangle$ (which means the "walker" starts at exact site N) and stays close to N during the whole evolution process, then we can use the approximation

$$\tilde{a} \approx \sum\sqrt{N}|n-1\rangle\langle n|, \tilde{a}^\dagger \approx \sum\sqrt{N}|n\rangle\langle n-1| \qquad (7)$$

to simplify the operators. The conditions on which this approximation holds will be discussed later. Then, assuming $\Delta\epsilon \approx 0$, we have

$$v = \Omega/2, \quad v' = g\sqrt{N}. \qquad (8)$$

Thus, when $v' < v$ ($\frac{\Omega/2}{g} > \sqrt{N}$) the average photon number upon measurement should be N (no change), and when $v' < v$ ($\frac{\Omega/2}{g} < \sqrt{N}$) the average photon number upon measurement should be $N-1$ (change of -1).

Due to the existence of decay term $-\frac{i\gamma}{2}|e\rangle\langle e|$ the Hamiltonian is not Hermitian. However, it satisfies the condition of parity-time symmetry, that is, after undergoing parity ($\hat{x} \to -\hat{x}, \hat{p} \to -\hat{p}$) and time reversal ($\hat{p} \to -\hat{p}, i \to -i$) transformation, the new Hamiltonian H' is only a constant away from the old Hamiltonian ($H' = H + cI$). Recent work [13] has proven that when we have $\frac{\Omega/2}{g} > \sqrt{N}$ the eigenvalues of the Hamiltonian are totally real, while when $\frac{\Omega/2}{g} < \sqrt{N}$ there is a pair of complex energy eigenvalues which correspond to unbroken and broken PT symmetries respectively.

As a key element of this experimental realization, a measurement of the photon number in the cavity needs to be carried out immediately after the qubit decays for the first time. One way to implement such a scheme is to prepare a low-decay qubit that is coupled to another resonator mode with big decay. By continuous measurement of that other resonator mode [24], which provides much of the qubit decay, one can observe such a decay immediately after it takes place, and thus carry out an energy measurement in the main resonator mode to retrieve the photon number.

III. ANALYTICAL THEORY

The analytical theory for this topological transition has been explained in detail [9]. Here we will extend their analytical theory to include the qubit dephase.

If the system is pure, one could use ψ_n^g to denote the amplitude at $|g\rangle \otimes |n\rangle$ and ψ_n^e at $|e\rangle \otimes |n\rangle$. In the presence

of dephase the density matrix of the system is mixed. We can similarly use the density matrix as $\rho^{g,g}_{n_1,n_2}(0) = \rho^{e,g}_{n_1,n_2}(0) = \rho^{g,e}_{n_1,n_2}(0) = 0$, $\rho^{e,e}_{n_1,n_2}(0) = \delta_{n_1,0}\delta_{n_2,0}$, where for $c,c' \in \{g,e\}$, $\rho^{c,c'}_{n_1,n_2}$ is the matrix entry corresponding to $|c\rangle\langle c'| \otimes |n_1\rangle\langle n_2|$. We have

$$\langle \Delta n \rangle = \sum_n n \cdot \left[\int_0^\infty \gamma \rho^{e,e}_{n,n}(t)\, dt \right]. \tag{9}$$

Then we translate this to momentum space by having

$$\rho^{c,c'}_{n,n'} = \frac{1}{(2\pi)^2} \oint dk \oint dk' e^{ikn} e^{-ik'n'} \rho^{c,c'}_{k,k'}. \tag{10}$$

This Hamiltonian becomes separable as for a 2×2 subspace of $|g/n\rangle \otimes |k\rangle$ we have

$$H_k = \begin{pmatrix} 0 & v_k \\ v_k^* & \Delta\epsilon - i\gamma/2 \end{pmatrix} \tag{11}$$

with $v_k = \frac{\Omega}{2} + g\sqrt{N}e^{-ik}$.

Using integration by part, we have that

$$n\rho^{e,e}_{n,n} = \frac{i}{(2\pi)^2} \oint dk \oint dk' e^{i(k-k')n} \partial_1 \rho^{e,e}_{k,k'}. \tag{12}$$

Summing over n and integrating over time, we have

$$\langle \Delta n \rangle = i\gamma \int_0^\infty dt \oint \frac{dk}{2\pi} \partial_1 \rho^{e,e}_{k,k}, \tag{13}$$

where we use $\partial_1 \rho^{e,e}_{k,k}$ as a shorthand of $\frac{\partial}{\partial k'} \rho^{e,e}_{k',k}|_{k'=k}$.

Now, one can define $p_k(t) := \rho^{g,g}_{k,k} + \rho^{e,e}_{k,k}$ as the probability that the subsystem of momentum k has not decayed till time t, with $\partial_t p_k = -\gamma \rho^{e,e}_{k,k}$. Also, one can use polar decomposition as $\rho^{e,e}_{k,k'}(t) = u_{k,k'}(t) \cdot e^{i\theta_{k,k'}(t)}$. With that, one can write

$$\begin{aligned} \langle \Delta n \rangle = \frac{i\gamma}{2\pi} \int_0^\infty dt \oint dk [& e^{i\theta_{k,k}(t)} \partial_1 u_{k,k}(t) \\ & + u_{k,k}(t) \cdot i \cdot e^{i\theta_{k,k}(t)} \cdot \partial_1 \theta_{k,k}(t)]. \end{aligned} \tag{14}$$

Considering the fact that $\theta_{k,k}(t) = 0$ as the diagonal terms of a density matrix are real, and $\partial_1 u_{k,k}(t) = \partial_2 u_{k,k}(t)$, one can find that the first term $e^{i\theta_{k,k}(t)} \partial_1 u_{k,k}(t)$ induces an integration of a closed contour and is thus zero. We can reach

$$\langle \Delta n \rangle = \frac{1}{2\pi} \int_0^\infty dt \oint dk [\partial_t p_k(t) \cdot \partial_1 \theta_{k,k}(t)]. \tag{15}$$

Defining

$$I_0 = \oint \frac{dk}{2\pi} \left[p_k \partial_1 \theta_{k,k}(t)|_0^\infty \right], \tag{16}$$

we have through integration by part

$$\langle \Delta n \rangle = I_0 - \int_0^\infty \oint \frac{dk}{2\pi} p_k \partial_t \partial_1 \theta_{k,k}(t). \tag{17}$$

Given the way we conduct Fourier transfer, we have $\rho_{k,k'} = \rho_{-k',-k}$, which means $\theta_{k,k'} = \theta_{-k',-k}$. Thus we have

$$\begin{aligned} \oint \frac{dk}{2\pi} p_k \partial_t \partial_1 \theta_{k,k}(t) &= -\oint \frac{dk}{2\pi} p_k \partial_t \partial_2 \theta_{-k,-k}(t) \\ &= \oint \frac{dk}{2\pi} p_k \partial_t \partial_2 \theta_{k,k}(t). \end{aligned} \tag{18}$$

Here we also use the fact that p_k is an even function in k. Given the fact that $\partial_1 \theta_{k,k}(t) + \partial_2 \theta_{k,k}(t) = 0$, that integration yields zero, and we have $\langle \Delta n \rangle = I_0$.

Given that the system eventually decays completely, $p_k(t \to \infty) = 0$, we have

$$\langle \Delta n \rangle = -\oint \frac{dk}{2\pi} \frac{\partial \theta_{k',k}(0)}{\partial k'}\bigg|_{k'=k}. \tag{19}$$

Since $\rho(0)$ is pure and diagonal in the basis of σ^z, for $\rho(\epsilon)$ considered up to the first order of $\epsilon \to 0^+$, one could find that the dephase term $d[\sigma^z \rho(t) \sigma^z - \rho(t)]$ does not affect $\rho(\epsilon)$ to the first order. Thus, by treating $\rho(\epsilon)$ as a pure state (which is similar to the case in Ref. [9]), we have

$$\langle \Delta n \rangle = -\oint \frac{dk}{2\pi} \frac{\partial \arg(-i v_k^*)}{\partial k}. \tag{20}$$

The topological structure is that, if $\Omega/2 > g\sqrt{N}$, then the integration of $-iv_k^*$ does not contain the axis origin and $\langle \Delta n \rangle = 0$; if $\Omega/2 < g\sqrt{N}$, then the integration of $-iv_k^*$ is an anticlockwise contour of a circle centered at $-i\Omega/2$ and with radius $g\sqrt{N}$, which contains the axis origin, thus $\langle \Delta n \rangle = -1$.

IV. NUMERICAL RESULTS AND DISCUSSIONS

We use a simple numerical integration technique to do the simulation. A MAXN = 320 [25] (which is the total dimension of the Hilbert space under consideration) dimensional complex vector V (matrix, if dephase is in consideration) is used to store the state of the system. In the absence of dephase, a matrix $U = e^{-i \cdot H \cdot t}$ is computed, and $U \cdot V$ simply yields the new state vector V. In the presence of qubit dephase we use the Lindblad master equation (6). Integration is carried out along the way until the amplitude of V converges [26]. The time interval t shrinks by half each time, and Richardson extrapolation is carried out until the final result converges.

Suppose one finds that when the qubit decays, the photon number in the resonator is n with probability P_n, we define

$$\langle N \rangle = \sum_{n=0}^{\infty} n P_n \tag{21}$$

to be the average photon number upon qubit decay.

A first glimpse of the results is provided in Fig. 2 with $N = 100$ [which is large, as proposed in Ref. [9] to meet the assumption of (7)]. Clear topological transition is observed if the system is initialized in a Fock state (black) ($|N\rangle$ in number basis).

Since Fock states with $N \gg 1$ are usually hard to prepare, we considered an alternative: a coherent state (Poisson distribution $\sum_k \frac{N^k e^{-N}}{k!} |k\rangle$ in number basis). However, the simulation (red line in Fig. 2) turns out to be quite similar in the case of noncoherent hopping (classical walker) despite large initial N. This shows that classical driving-induced coherent states cannot be used for this topological transition.

Considering the fact that Fock states with $N \gg 1$ are hard to come by, we relax that condition and examine some cases with small Fock numbers. An extreme case of $N = 1$ is displayed in Fig. 3(a), which still preserves the basic traits of a topological transition despite the small initial Fock number.

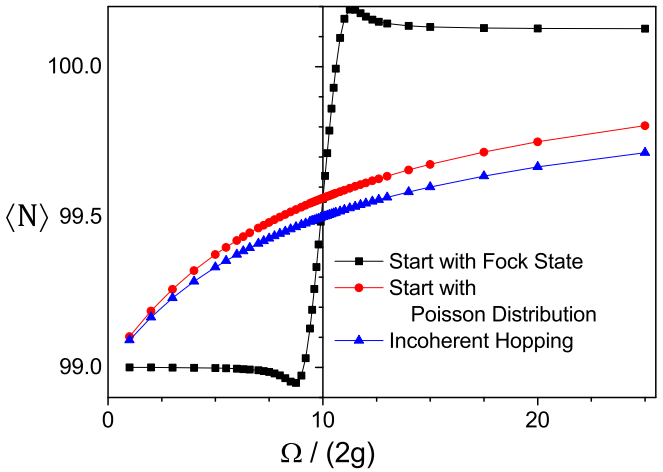

FIG. 2. Results of a non-Hermitian quantum walk for $N = 100$ with different starting distributions (Poisson and Fock) of the resonator and comparison with classical incoherent hopping. The variable $\Omega/2g$ captures the relative strengths of inter- and intra-unit hopping in the quantum walk, and $\langle N\rangle$ is the average photon number upon qubit decay. The other parameters are $g = 1$ (set as a benchmark), $\gamma = 4$, $\Delta\epsilon = 10^{-4}$ while Ω varies. For classical incoherent hoppings, we used the result of Eq. (2).

Further investigation into the problem yields Fig. 3(b), which shows that the curve for different N overlap.

A. Different decay factors and energy-level differences

In this section we consider the effect of qubit decay factors γ and detuning $\Delta\epsilon$ on this experiment.

In theory [9], qubit decay factor γ affects only the (expected) evolution time, not the topological transition, so the expected result should be the same for different γ. We run a simulation for different initial N with identical parameters like g and $\Delta\epsilon$ for different decay factors γ, with the result in Fig. 4. We observe that the qubit decay factor γ cannot be too small (at least $\gamma > g$ should be satisfied), otherwise the photon number upon measurement would be too large. This is necessary for both small and large N.

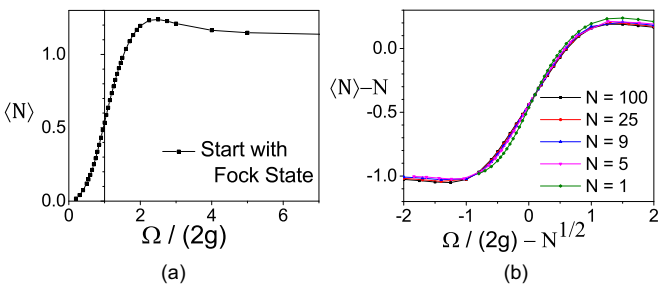

FIG. 3. Results of simulation for non-Hermitian quantum walk with small initial N and comparison. (a) The variable $\Omega/2g$ captures the relative strengths of inter- and intra-unit hopping in the quantum walk, and $\langle N\rangle$ is the average photon number upon qubit decay. (b) Those two variables are compared against topological transition threshold $\sqrt{N}$ and initial photon number N, respectively. The parameters in both figures are (same as Fig. 2) $g = 1$, $\gamma = 4$, $\Delta\epsilon = 10^{-4}$ while Ω varies.

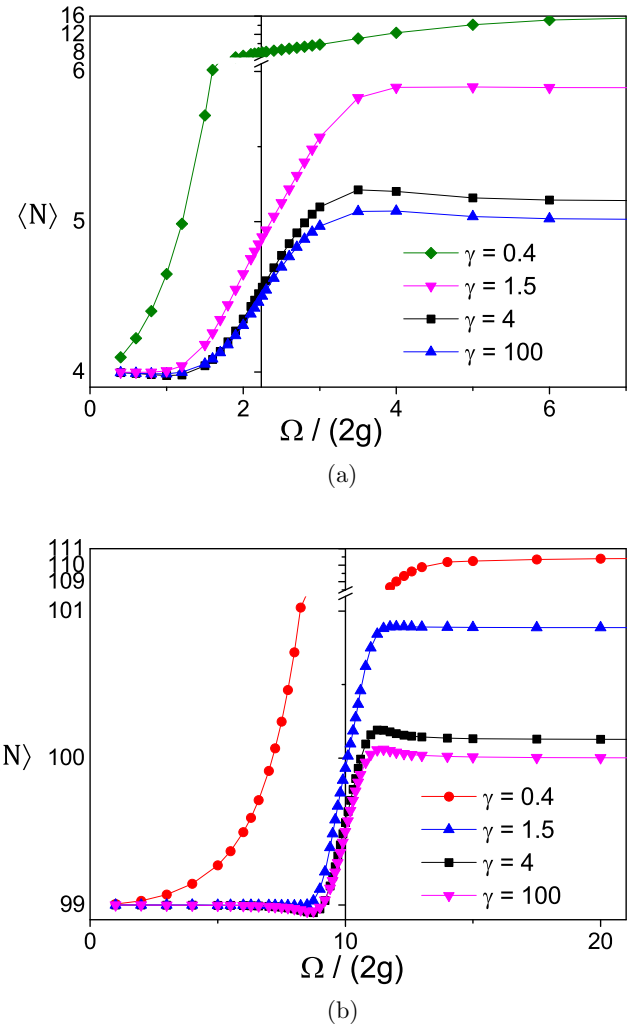

FIG. 4. Results of simulation for non-Hermitian quantum walk with different qubit decay factor γ under (a) initial $N = 5$ and (b) initial $N = 100$. The variable $\Omega/2g$ captures the relative strengths of inter- and intra-unit hopping in the quantum walk, and $\langle N\rangle$ is the average photon number upon qubit decay. The other parameters are $g = 1$, $\Delta\epsilon = 10^{-4}$ while Ω varies. One can observe that if qubit decay factor γ is small, the curve significantly deviates from theoretical deduction, while for large γ, the curves converge.

The difference between analytical theory and numerical results lies in the assumption of Eq. (7), which is valid only if the system stays close to photon number N throughout the whole evolution. If decay factor γ is small, the quantum walker can walk far away from the initial site, overturning that assumption. Specifically, since we have

$$\tilde{a} = \sum_n \sqrt{n}\,|n-1\rangle\langle n|\,, \tilde{a}^\dagger = \sum_n \sqrt{n}\,|n\rangle\langle n-1|\,, \qquad (22)$$

the strengths of intersite hoppings grow stronger as the site number (or energy level in our simulation) increases, which explains why for small γ the curves deviate significantly to higher energy levels.

Luckily, big γ does not present an experimental difficulty in reality, as big qubit decays are usually easy to generate. We found that $\gamma = 4$ (four times the coupling strength) is roughly

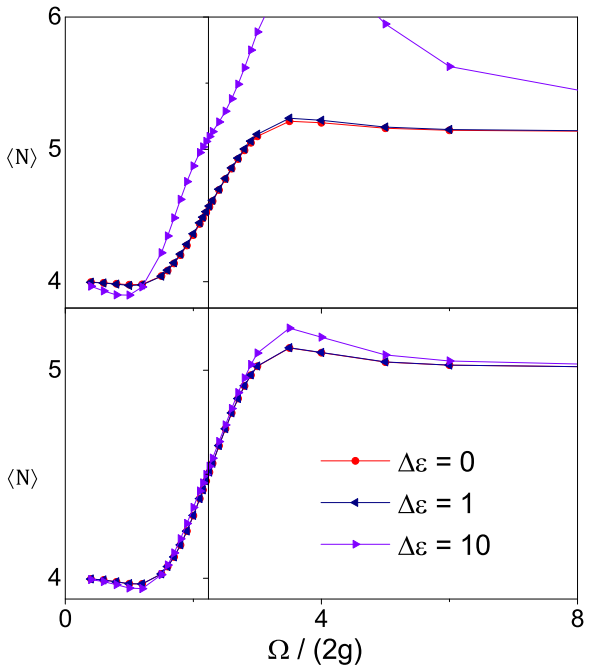

FIG. 5. Results of simulation for non-Hermitian quantum walk with different system detuning $\Delta\epsilon$ under initial $N = 5$, with (upper) under qubit decay $\gamma = 4$ and (lower) $\gamma = 20$. Notice that the difference between $\Delta\epsilon = 1$ and $\Delta\epsilon = 0$ in (lower) is so tiny that one can barely distinguish them in the plot. The variable $\Omega/2g$ captures the relative strengths of inter- and intra-unit hopping in the quantum walk, and $\langle N\rangle$ is the average photon number upon qubit decay. The other parameter is $g = 1$ while Ω varies.

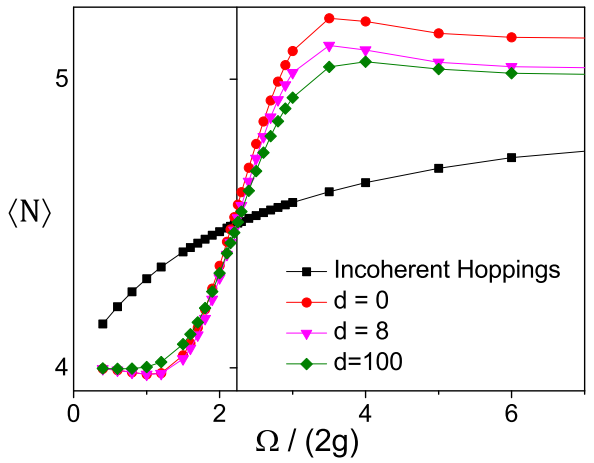

FIG. 6. Results of simulation for non-Hermitian quantum walk with different qubit dephase rate d under initial $N = 5$. The variable $\Omega/2g$ captures the relative strengths of inter- and intra-unit hopping in the quantum walk, and $\langle N\rangle$ is the average photon number upon qubit decay. The parameters are (same as Fig. 2) $g = 1, \gamma = 4$, $\Delta\epsilon = 10^{-4}$ while Ω varies.

where qubit decay rate starts to negatively affect the observed topological transition, so we will stick to this value henceforth.

Figure 5 shows the effect of detuning on this experiment. Ideally we want $\Delta\epsilon = 0$, which is an exact match to the quantum walk scenario. Simulation shows that as long as the detuning of the system is kept small (Fig. 5 shows that $\Delta\epsilon < g, \Omega$ suffices), it will not have a tangible effect on the result of this experiment.

It's worthwhile to notice that in theory, neither $\Delta\epsilon$ nor γ should affect the experimental results. Yet in Fig. 5, one can observe that for a fixed $\Delta\epsilon = 10$, increasing qubit decay γ yields better topological transition. We believe approximation (7) plays a major role here, just like in Fig. 4, as small qubit decay γ yields a wider amplitude span to overturn approximation (7).

B. Dephasing effects

Dephasing characterizes one major effect of noise on circuit QED systems, making a quantum system less "quantum" but more "classical." Here we consider dephase of the qubit due to external field fluctuation, which is one of the major sources of dephase in a circuit QED system, and can be written in Lindblad master equation (6), where d characterizes the strength of such dephase. Such dephase keeps the diagonal elements of ρ, but in addition to other standard evolution the nondiagonal elements of it shrink exponentially by $e^{-d\cdot t}$. Here we run a numerical simulation where qubit decay rate γ and other parameters like g, $\Delta\epsilon$ are kept identical for different qubit dephase factor d.

The results are seen in Fig. 6, which shows that the topological transition grows less distinct as the qubit dephase factor d grows. Yet even when the dephase of the qubit is very large ($d = 100$) compared with the other elements of the system $\Omega, \gamma, g < 10$, good topological transition can still be observed, as compared to the classical incoherent hopping.

The numerical results agree with the analytical theory which we put forward earlier in this paper. This topological structure is well protected from the dephase. No matter how much dephase we have in the system, as long as such dephase comes from external field fluctuation, and can be treated as Markovian in the time scale of other operations in the system, it will not affect experimental results.

V. TWO-DIMENSIONAL QUANTUM WALK AND ITS REALIZATION IN A CIRCUIT QED SYSTEM

In this section we extend the 1D quantum walk to higher dimensions. We first consider the 2D case. Here each unit still consists of a decaying site and a nondecaying site; however, a "walker" could make interunit hopping in two dimensions, with their strengths characterized by v' and v'' each. The strength of hopping between two sites of the same unit is still v. Figure 7 provides a sketch of the model.

In a circuit QED system, it is relatively easy to accommodate this change by adding a second resonator mode coupled to the qubit. Like before, if one uses $|e/g\rangle \otimes |n_1\rangle \otimes |n_2\rangle$ to identify the state of the system, then the Hamiltonian of the system is

$$H = g_1(\sigma^+\tilde{a_1} + \sigma^-\tilde{a_1}^\dagger) + g_2(\sigma^+\tilde{a_2} + \sigma^-\tilde{a_2}^\dagger) + \Omega/2(\sigma^+ + \sigma^-) + \frac{1}{2}\Delta\epsilon\sigma^z - \frac{1}{2}\frac{i\gamma}{2}|e\rangle\langle e|, \quad (23)$$

where σ are still Pauli operators on the qubit, and $\tilde{a_{1/2}}$ are lowering and rising operators on the first or second resonator

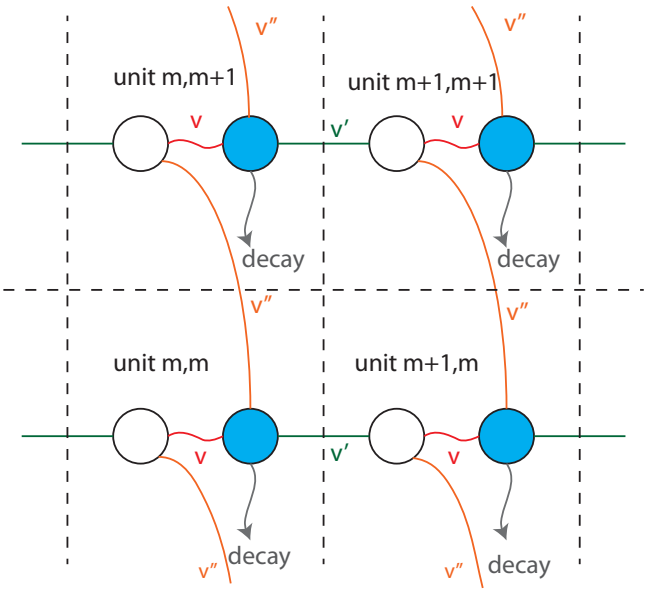

FIG. 7. Two-dimensional quantum walk model. The system is similar to the one in Fig. 1, except with one more dimension. Three colors (red, orange, and green) are used to distinguish different kinds of hopping (red for intrasite, orange and green for intersite on two different dimensions). The dashed lines are used to indicate the boundaries of each site.

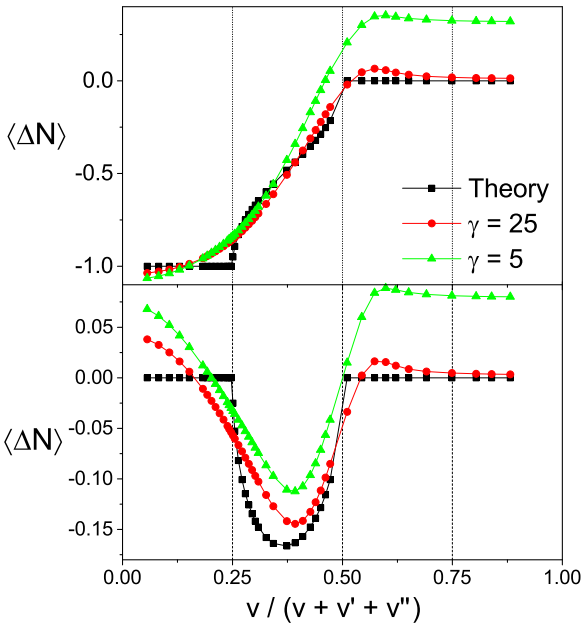

FIG. 8. 2D Hoppings: Results of simulation with different qubit decay factor γ under initial $N = 5$ and comparison with the theoretical (ideal) case for a two-dimensional walk in (upper) the first resonator mode and (lower) the second resonator mode. The coupling strengths are set to $g_1 = 2$, $g_2 = 1$ to satisfy constraint $v'/v'' = 2$. The independent variable is calculated by $v/(v + v' + v'') := \Omega/[\Omega + 2\sqrt{N}(g_1 + g_2)]$ to fit in the form of Eq. (27). $\langle \Delta N\rangle := \langle N\rangle - N$ is the average photon number change upon qubit decay in each resonator mode. The other parameter is $\Delta\epsilon = 10^{-4}$ while Ω varies. From the fact that a similar qubit decay ($\gamma = 5$) as one-dimensional hoppings leads to a large deviation from the ideal topological structure one can observe that a larger qubit decay is necessary for 2D experiments.

field in a rotating frame, $\Delta\epsilon$ is (real) detuning of the system, and γ is the decay rate of the excited qubit state.

A. Analytical theory for higher-dimensional quantum walk

The theory for a higher-dimensional case without dephase has been explained in Ref. [11], which is a simple extension of the 1D case, and so the following section considers dephase.

Suppose the dimension is d. As in the 1D case, one can still use $\rho^{c,c'}_{\mathbf{n},\mathbf{n}'}$ to denote the state of the system, where $\mathbf{n}$ and $\mathbf{n}'$ are d-dimensional vectors and $c,c' \in \{g,e\}$. The same Fourier translation into momentum space yields that for subspace $\mathbf{k}$,

$$H_{\mathbf{k}} = \begin{pmatrix} 0 & \mathbf{A}_{\mathbf{k}} \\ \mathbf{A}_{\mathbf{k}}^{*} & \Delta\epsilon - i\hbar\gamma/2 \end{pmatrix}, \tag{24}$$

with $\mathbf{A}_{\mathbf{k}} = \frac{\Omega}{2} + \sum_{\alpha=1}^{d} g^{(\alpha)}\sqrt{N}e^{-ik_\alpha}$. Defining $p_{\mathbf{k}}(t)$ in the same way as

$$p_{\mathbf{k}} = \rho^{g,g}_{\mathbf{k},\mathbf{k}} + \rho^{e,e}_{\mathbf{k},\mathbf{k}} \tag{25}$$

and with $\partial_t p_{\mathbf{k}} = -\gamma\psi^{e,e}_{\mathbf{k},\mathbf{k}}(t)$ and integrating by part, one can reach

$$\langle \Delta n_\alpha\rangle = \oint \frac{d^{d-1}k}{(2\pi)^{d-1}}\left\{ i\gamma \int_0^\infty dt \oint \frac{dk_\alpha}{2\pi}\partial_{k_\alpha,1}\rho^{e,e}_{\mathbf{k},\mathbf{k}}\right\}, \tag{26}$$

while the shorthand $\partial_{k_\alpha,1}$ means taking partial derivative only on the αth component of $\mathbf{k}$, and only on the first $\mathbf{k}$ in the density matrix. It is not hard to see that the expression inside the brace is exactly as Eq. (13) and thus is either 0 or 1, no matter what dephasing factors we have.

Now, if one comes back to the definition of $\mathbf{A}_{\mathbf{k}} = \frac{\Omega}{2} + \sum_{\alpha=1}^{d} g^{(\alpha)}\sqrt{N}e^{-ik_\alpha}$, one way to understand Eq. (26) is to first fix $d-1$ angles $k_{\beta\neq\alpha}$, then see whether the integration of k_α from 0 to 2π would cause the angle of $\mathbf{A}_{\mathbf{k}}$ to also shift 2π, and then integrate over those $d-1$ angles. During the integration of the other $d-1$ angles, we may observe new topological structures, like the middle area of Fig. 8, with some old traits still remaining, like the two sides of Fig. 8.

For the 2D case that is relatively easy to simulate, assuming $g_1 > g_2$, the results are

$$\langle \Delta n_1\rangle = \begin{cases} -1 \\ -1 + \frac{\theta_1}{\pi}, \\ 0 \end{cases} \qquad \langle \Delta n_2\rangle = \begin{cases} 0 & v' > v + v'' \\ -\frac{\theta_2}{\pi} & |v - v'| \leqslant v'', \\ 0 & v' < v - v'' \end{cases} \tag{27}$$

with $\cos\theta_1 = \frac{N(g_1^2 - g_2^2) - \Omega^2/4}{\Omega\sqrt{N}g_2}$, $\cos\theta_2 = \frac{N(g_1^2 - g_2^2) + \Omega^2/4}{\Omega\sqrt{N}g_2}$, $v = \Omega/2$, $v' = \sqrt{N}g_1, v'' = \sqrt{N}g_2$ in this system.

B. Numerical results

We run numerical simulations for the 2D case in a similar manner as for the 1D case, except that the tensor product of two vectors is stored. We truncated photon number at MAXN = 20 with hindsight knowledge from the 1D simulations. From Fig. 8 one can see that the results of the simulation preserve the basic properties of a 2D transition. It also shows that in the 2D case, a more stringent requirement is put onto the system

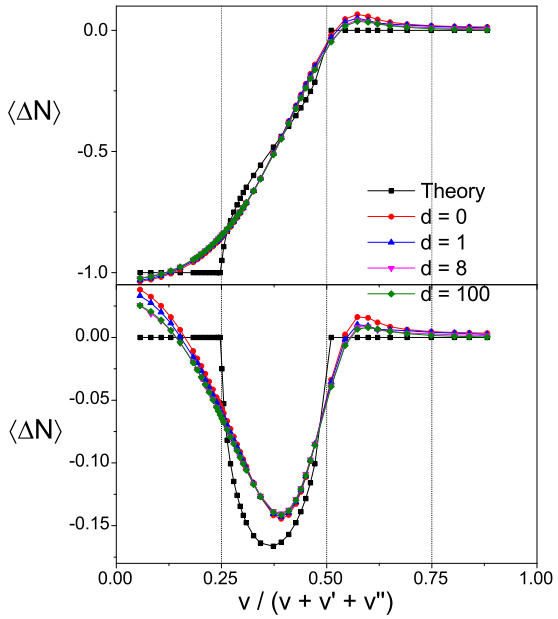

FIG. 9. 2D hoppings: Results of simulation with different dephase factor d for the qubit under initial $N = 5$, and comparison with the theoretical (ideal) case for a 2D walk in (upper) the first resonator mode and (lower) the second resonator mode. The coupling strengths are set to $g_1 = 2, g_2 = 1$ to satisfy constraint $v'/v'' = 2$. The independent variable is calculated by $v/(v + v' + v'') := \Omega/[\Omega + 2\sqrt{N}(g_1 + g_2)]$ to fit in the form of Eq. (27). $\langle \Delta N \rangle := \langle N \rangle - N$ is the average photon number change upon qubit decay in each resonator mode. The other parameters are $\gamma = 25$, $\Delta\epsilon = 10^{-4}$ while Ω varies. From the fact that the curves for different dephase factor d almost overlap one can see that the qubit dephase factor does not affect the simulated result.

as a much bigger decay factor γ is necessary to preserve the topological nature of the system compared to the 1D case.

We have also numerically simulated the effect of qubit dephase on the final result. Using a similar method in Sec. IV B, we simulated Eq, (6) exactly and displayed the results in Fig. 9, which shows that different qubit dephase factor d does not affect our result.

Due to the fact that analytical theory for different dimensions follows similar integration over contours, we expect that in a higher dimensional case, the topological effect would still be protected from qubit dephase.

VI. CONCLUSION

In summary, we considered the quantum walk on a 1D bipartite indexed lattice, where each unit has one decay site and one nondecay site. We have proved the topological transition of average decay site in this non-Hermitian system is not affected by either the decay or the dephasing between sites within units.

We proposed a circuit QED model where a qubit is coupled to one resonator mode. We have numerically shown that such topological transition in a non-Hermitian quantum walk can be realized in this system. We numerically proved that neither large decay nor dephase of the qubit would affect the topogical transition. In fact, we found that the qubit decay should be larger than g, in order to maintain the topological transition. We extended this circuit QED implementation to higher dimension quantum bipartite walks showing the features that arise with higher dimensionality.

ACKNOWLEDGMENTS

We thank L. Sun for helpful discussions. This work is funded by the National Basic Research Program of China (973 Program) 2011CBA00300 (2011CBA00301), National Natural Science Foundation of China Grants No. 61435007, No. 11574353, No. 11274351, and No. 11474177.

APPENDIX: DETAILED DEDUCTION FROM QUANTUM JUMP TO NON-HERMITIAN HAMILTONIAN

As with our main text, we assume that qubit decay and qubit dephase are the only sources of decoherence in the system. While qubit dephase is undetectable from photon detectors, qubit decay can be detected with leaking photon. For our specific system, we followed the procedure adopted in quantum-jump simulations [22,27,28] for our system.

Suppose the system starts in state ρ. In order to determine the evolution of the system, we take these steps:

1. Determine the current probability of a qubit decay over an infinitesimally small time Δt:

$$\Delta P = \gamma \Delta t Tr[\sigma^- \rho \sigma^+].$$

2. Obtain a random number r between zero and one, compare with ΔP, and decide on emission using the following steps.

3. If $r < \Delta P$, there is an emission, so that the system jumps to the renormalized form

$$\rho \to \frac{\sigma^- \rho \sigma^+}{Tr[\sigma^- \rho \sigma^+]}. \tag{A1}$$

4. If $r > \Delta P$, no emission takes place, so the system evolves under original Hamiltonian, without the decay term

$$\rho \to \rho - i[H_{\rm org}, \rho]\Delta t + d\Delta t(\sigma^z \rho \sigma^z - \rho). \tag{A2}$$

5. Repeat to obtain an individual trajectory or history.

6. Average observables over many such trajectories.

We know that the system splits into two alternatives in a time Δt, that is, into $\rho_{\rm decay}$ with probability ΔP and into $\rho_{\rm no-decay}$ with probability $1 - \Delta P$. To show that the non-Hermitian Hamiltonian has the same effect as the system as master equation, we consider the evolution of the total density matrix, as ρ evolves into

$$\Delta P \rho_{\rm decay} + (1 - \Delta P)\rho_{\rm no-decay} \tag{A3}$$

$$= \gamma \Delta t {\rm Tr}[\sigma^- \rho \sigma^+] \frac{\sigma^- \rho \sigma^+}{{\rm Tr}[\sigma^- \rho \sigma^+]} + (1 - \gamma \Delta t {\rm Tr}[\sigma^- \rho \sigma^+]) \times [\rho - i[H_{\rm org}, \rho]\Delta t + d\Delta t(\sigma^z \rho \sigma^z - \rho)] \tag{A4}$$

$$\approx \rho - i[H_{\rm org}, \rho]\Delta t + d\Delta t(\sigma^z \rho \sigma^z - \rho) + \gamma \Delta t(\sigma^- \rho \sigma^+ - \rho {\rm Tr}[\sigma^- \rho \sigma^+]). \tag{A5}$$

Since we have

$$\rho Tr[\sigma^- \rho \sigma^+] = \sigma^+\sigma^-\rho = \rho\sigma^+\sigma^-, \tag{A6}$$

one can see that this is exactly how the system would evolve under master equation (4).

On the other hand, in Eq. (A2), one can see that with a non-Hermitian Hamiltonian

$$H = H_{\text{org}} - \frac{i\gamma}{2}\sigma^+\sigma^- \tag{A7}$$

and the relation in Eq. (A6) we have

$$\begin{aligned}(1 - \gamma\Delta t \text{Tr}[\sigma^-\rho\sigma^+])\{\rho - i[H_{\text{org}},\rho]\Delta t + d\Delta t(\sigma^z\rho\sigma^z - \rho)\} \\ \approx \rho - i[H,\rho]\Delta t + d\Delta t(\sigma^z\rho\sigma^z - \rho),\end{aligned} \tag{A8}$$

where the approximation holds in the first order of Δt. The left-hand side is just Eq. (A2) and multiplies the probability that the qubit does not decay; the right-hand side is evolution under the non-Hermitian Hamiltonian. This shows the non-Hermitian Hamiltonian H characterizes the evolution of the system given that the qubit does not decay and the probability of that. So in our paper we used

$$\dot{\rho}(t) = -i[H,\rho(t)] + d[\sigma^z\rho(t)\sigma^z - \rho(t)] \tag{A9}$$

to characterize the evolution of the system.

[1] M. Szegedy, Quantum Speed-Up of Markov Chain Based Algorithms, in *Proceedings of the 45th IEEE Symposium on Foundations of Computer Science* (IEEE, New York, 2004), pp. 32–41.

[2] A. M. Childs, Universal Computation by Quantum Walk, Phys. Rev. Lett. **102**, 180501 (2009).

[3] Z. H. Bian, J. Li, H. Qin, X. Zhan, R. Zhang, B. C. Sanders, and P. Xue, Realization of Single-Qubit Positive-Operator-Valued Measurement via a One-Dimensional Photonic Quantum Walk, Phys. Rev. Lett. **114**, 203602 (2015).

[4] A. Ambainis, E. Bach, A. Nayak, A. Vishwanath, and J. Watrous, One-dimensional quantum random walk, in *Proceedings of the 33rd Annual AMC Symposium on Theory of Computing* (ACM Press, New York, 2001), pp. 37–49.

[5] Gregory S. Engel *et al.*, Evidence for wavelike energy transfer through quantum coherence in photosynthetic systems, Nature (London) **446**, 782 (2007).

[6] M. Mohseni *et al.*, Environment-assisted quantum walks in photosynthetic energy transfer, J. Chem. Phys. **129**, 174106 (2008).

[7] Qing Ai, Tzu-Chi Yen, Bih-Yaw Jin, and Yuan-Chung Cheng, Clustered geometries exploiting quantum coherence effects for efficient energy transfer in light harvesting, J. Phys. Chem. Lett. **4**, 2577 (2013).

[8] Qing Ai, Yuan-Jia Fan, Bih-Yaw Jin, and Yuan-Chung Cheng, An efficient quantum jump method for coherent energy transfer dynamics in photosynthetic systems under the influence of laser fields, New J. Phys. **16**, 053033 (2014).

[9] M. S. Rudner and L. S. Levitov, Topological Transition in a Non-Hermitian Quantum Walk, Phys. Rev. Lett. **102**, 065703 (2009).

[10] C. M. Bender, Making Sense of Non-Hermitian Hamiltonians, Rep. Prog. Phys. **70**, 947 (2007).

[11] M. S. Rudner and L. S. Levitov, Phase transitions in dissipative quantum transport and mesoscopic nuclear spin pumping, Phys. Rev. B **82**, 155418 (2010).

[12] A simple explanation based on the first decay site of the walker is as follows: with probability $\frac{v}{v'+v}$ the first decay site of the walker is on the same unit, with probability $\frac{v'}{v'+v}$ the first decay site of the walker is on the previous unit. Once a walker is on a decay site, the average decay site from then on is just that unit based on the symmetry of the system. So the average displacement would be $-\frac{v'}{v'+v}$.

[13] S. Longshi, Convective and absolute PT-symmetry breaking in tight-binding lattices, Phys. Rev. A **88**, 052102 (2013).

[14] C. M. Bender and S. Boettcher, Real Spectra in Non-Hermitian Hamiltonians Having PT Symmetry, Phys. Rev. Lett. **80**, 5243 (1998).

[15] C. E Rüter *et al.*, Observation of parity-time symmetry in optics, Nature Phys. **6**, 192 (2010).

[16] L. Chang, X. Jiang, S. Hua, C. Yang, J. Wen, L. Jiang, G. Li, G. Wang, and M. Xiao, Parity-time symmetry and variable optical isolation in active-passive-coupled microresonators, Nature Photonics **8**, 524 (2014).

[17] H. Walther, B. T. H. Varcoe, B.-G. Englert, and T. Becker, Cavity quantum electrodynamics, Rep. Prog. Phys. **69**, 1325 (2006).

[18] Zhang-qi Yin and Fu-li Li, Multiatom and resonant interaction scheme for quantum state transfer and logical gates between two remote cavities via an optical fiber, Phys. Rev. A **75**, 012324 (2007).

[19] A. Blais, J. Gambetta, A. Wallraff, D. I. Schuster, S. M. Girvin, M. H. Devoret, and R. J. Schoelkopf, Quantum-information processing with circuit quantum electrodynamics, Phys. Rev. A **75**, 032329 (2007).

[20] J. M. Zeuner, M. C. Rechtsman, and Y. Plotnik, Observation of a Topological Transition in the Bulk of a Non-Hermitian System, Phys. Rev. Lett. **115**, 040402 (2015).

[21] M. Reagor, H. Paik, G. Catelani, L. Sun, C. Axline, E. Holland, I. M. Pop, N. A. Masluk, T. Brecht, L. Frunzio, M. H. Devoret, L. Glazman, and R. J. Schoelkopf, Reaching 10 ms single photon lifetimes for superconducting aluminum cavities, Appl. Phys. Lett. **102**, 192604 (2013).

[22] M. B. Plenio and P. L. Knight, The quantum Cjump approach to dissipative dynamics in quantum, Rev. Mod. Phys. **70**, 101 (1998).

[23] H. M. Wiseman and G. J. Milburn, *Quantum Measurement and Control* (Cambridge University Press, Cambridge, 2009).

[24] L. Sun, A. Petrenko, Z. Leghtas, B. Vlastakis, G. Kirchmair, K. M. Sliwa, A. Narla, M. Hatridge, S. Shankar, J. Blumoff, L. Frunzio, M. Mirrahimi, M. H. Devoret, and R. J. Schoelkopf, Tracking photon jumps with repeated quantum

non-demolition parity measurements, Nature (London) **511**, 444 (2014).

[25] With hindsight we only need the dimension of Hilbert space for the resonator to be $2N$, which means MAXN $\sim 4N$ is simply enough. Choosing such a large number is to make sure that we do not need to change the configuration of the system for different initial Fock state numbers like $N = 1$ and $N = 100$.

[26] Due to the existence of "dark state" for finite systems, that amplitude will not go to exactly zero.

[27] J. Dalibard, Y. Castin, and K. Mølmer, Wave-Function Approach to Dissipative Processes in Quantum Optics, Phys. Rev. Lett. **68**, 580 (1992).

[28] R. Dum, P. Zoller, and H. Ritsch, Monte Carlo simulation of the atomic master equation for spontaneous emission, Phys. Rev. A **45**, 4879 (1992).